



PERGAMON

Chemical Engineering Science 56 (2001) 4205–4216

Chemical
Engineering Science

www.elsevier.com/locate/ces

Simulations of the structure and properties of amorphous silica surfaces

Jeanette M. Stallons, Enrique Iglesia *

Department of Chemical Engineering, University of California at Berkeley, Berkeley, CA 94720, USA

Received 10 December 1999; accepted 26 December 2000

Abstract

The structure and transport properties of solid surfaces have been described using models of varying complexity and rigor without systematic comparisons among available methods. Here, we describe the surface of amorphous silica using four techniques: (1) an ordered surface created by cutting the structure of a known silica polymorph (α -cristobalite); (2) an unrelaxed amorphous surface obtained by cutting bulk amorphous silica structures created by molecular dynamics methods; (3) a relaxed amorphous surface created by relaxing the amorphous surface; and (4) a random surface created by Monte Carlo sphere packing methods. Calculations of the adsorption potential surface and simulation of the surface diffusion of weakly bound adsorbates (N_2 , Ar, CH_4) interacting via Lennard–Jones potentials with these surfaces were used to compare surface models and to judge their fidelity by comparisons with available experimental values. Similar heats of adsorption were obtained on the relaxed, unrelaxed, and random surfaces (± 0.5 kJ/mol), but the relaxed surface showed greater heterogeneity with a wider distribution of adsorption energies. Surface diffusion on the relaxed surface was slower than on the other surfaces, with slightly higher activation energies (0.5–1.0 kJ/mol). Rigorous comparisons between simulated and experimental surface diffusivities are not possible, because of scarce surface diffusion data on well-characterized surfaces. The values obtained from simulations on silica were similar to experimental surface diffusivities reported on borosilicate glasses. © 2001 Published by Elsevier Science Ltd.

Keywords: Porous media; Simulation; Transport processes; Diffusion; Surface diffusion; Adsorption

1. Introduction

Simulations are increasingly useful tools in the design of porous solids by helping to understand and to predict the structure and transport properties of these solids (MacElroy & Raghavan, 1991; Reyes & Iglesia, 1993; Drewry & Seaton, 1995; Keil, 1996). Most surface models, however, neglect the details of the surface structure and they adopt instead the pragmatic approach of describing surfaces using simple lattice models with mathematically convenient distributions of binding sites. A systematic study of how these approaches lead to varying degrees of accuracy, fidelity, and predictive value appears to be currently unavailable. Here, we attempt such a systematic comparison by describing surface structures using several methods, differing in approach and level of complexity, and comparing their ability to predict

the adsorption and surface diffusion properties of amorphous silica. Amorphous solids are used because they pose more formidable simulation challenges than known and well-defined crystalline structures. Silica was chosen as an example because of its widespread use as adsorbents, catalyst supports, and porous membranes. Several previous studies of the bulk and surface structures of amorphous solids have been carried out on silica and the required interatomic potentials are available from these studies (Feuston & Garofalini, 1989, 1990; Athanasopoulos & Garofalini, 1992; Kohler & Garofalini, 1994; Litton & Garofalini, 1997).

Recent studies have introduced heterogeneity into simple lattice models in order to attempt to describe the chemical non-uniformity of amorphous surfaces. For example, adsorption energy distributions were assigned to various available lattice sites (Nicholson & Silvester, 1977; O'Brien & Myers, 1985). Surface features, such as steps, terraces, holes, or grooves have been placed on square lattices (Haus & Kehr, 1987; Bojan & Steele,

* Corresponding author. Tel.: +1-510-642-9673. fax: +1-510-642-4778.

E-mail address: eiglesia@aol.com (E. Iglesia).

1988; Gomer, 1990; Rudzinski & Everett, 1992; Steele, 1997; Zgrablich, 1997). The smaller holes and barriers are distributed randomly on the surfaces; the larger dimensions and spacing of the steps and grooves are approximated from experimental microscopy data (Gomer, 1990; Steele, 1997). Disorder of the underlying surface structure itself has been introduced using lattices with more complex topology, for example, by perturbing all vertex positions in a square lattice by a random displacement vector (Benegas, Pereyra, & Zgrablich, 1987). These approaches retain the assumption that random, heterogeneous surfaces can be described by distributions of sites on regular or distorted ordered structures, without including the detailed topological connectivity among surface atoms or between surface atoms and the bulk atoms immediately below. Nevertheless, it seems that connectivity and interactions with sub-surface atoms should influence strongly the transport and binding properties of these amorphous surfaces.

Bakaev and Steele (1992) used a “Bernal surface” (Finney, 1983), created by randomly packing spheres, representing oxygen atoms, within a three-dimensional container with periodic boundary conditions using Monte Carlo methods. The sphere size was set as the diameter of lattice oxygen anions. Riccardo and Steele (1996) used this Bernal surface to simulate Ar surface diffusion on amorphous titania. The interactions of Ar with surface oxygens were described by Lennard–Jones potentials parameterized by comparing experimental and simulated adsorption isotherms. Surface “roughness” was varied by random removal of some surface spheres; the resulting “roughness” had a marked effect on surface transport rates at low temperatures (85–160 K). For example, diffusion activation energies increased from 4.7 to 7.1 kJ/mol as three monolayers of atoms were randomly removed from the initial Bernal surface. Fractal dimensions (D_f) of 2.2–2.5 were calculated from the effects of the diameter of the adsorbates on the maximum achievable coverage (monolayer capacity) on various simulated surfaces. The approximate agreement observed between these and experimental fractal dimensions for silica surfaces ($D_f = 2.03$ – 2.30) was taken as evidence of the fidelity of the simulation approach. The activation energies and surface diffusivities obtained in these simulations on roughened Bernal surfaces were not compared with experimental results.

Clearly, atoms on surfaces are not located at random positions but at positions of minimum energy, and these positions are not static but they relax both after the surface is first formed by fracturing, abrupt termination of particle growth, or cooling from melts, and during adsorption and diffusion of molecules. The forces among surface atoms, those in subsurface regions, and those in adsorbed molecules can be described accurately by empirical potential energy functions parametrized to describe the bulk structural details of amorphous solids (e.g.

radial structure functions and bond angle distributions). The choice of potential energy function is critical, because it determines the positions of atoms at the surface. Few studies have included this level of detail in describing surfaces. Garofalini et al. have examined the structure of silica surfaces (Feuston & Garofalini, 1989; Athanaspoulos & Garofalini, 1992; Kohler & Garofalini, 1994) and the surface diffusion of silicon and oxygen lattice atoms at high temperatures (Litton & Garofalini, 1997). Bakaev (1999) and Bakaev and Steele (1999a, b) have recently addressed the incomplete surface annealing in the Garofalini methods, which leads to pendant oxygens suggested to account for OH groups experimentally found at the surface of silica. These authors proposed that hydrophobic silica surfaces require the substantial absence of OH groups and require much higher annealing temperatures in the structural simulations of the surface. Silica surfaces used as adsorbents and as catalyst supports, however, contain significant OH surface densities; thus, the Garofalini method appears to be more realistic in the simulation of silica surfaces formed by abrupt termination of particle growth in aqueous media followed by thermal treatments at temperatures well below the glass transition temperature. MacElroy and Raghavan (1990, 1991) explored the diffusion of methane and silicon hexafluoride within random microporous silicas. Both groups used molecular dynamics or Monte Carlo simulations to place Si and O atoms accurately within bulk silica and then created a surface by cutting and, in some cases, relaxing the bulk structure.

In this study, various silica surfaces were created and their adsorption and transport properties were compared with one another and with available experimental results in order to assess the level of detail required for the faithful representations of these heterogeneous random surfaces. Specifically, surfaces were created by simple or relaxed cuts of simulated bulk silica (unrelaxed and relaxed surfaces, respectively) and by Monte Carlo packing methods (random surface). The properties of these amorphous surfaces were compared with those of ordered systems, in which uniform adsorption sites are placed in a lattice corresponding to α -cristobalite, a crystalline silica polymorph (ordered surface). Both the thermodynamics of adsorption and the dynamics of surface transport of weakly bound adsorbates are simulated.

2. Bulk silica simulation

2.1. Method

Bulk silica was described using well-established molecular dynamics techniques (Woodcock, Angell, & Cheeseman, 1976; Soules, 1979; Garofalini & Melman, 1986; Feuston & Garofalini, 1988). Simulations were carried out using methods described by Feuston and

Garofalini (1988). Atoms were placed in initial configurations of α -cristobalite, β -cristobalite, α -quartz, or in an arbitrary regular structure with four oxygen atoms around each silicon atom. Initial velocity components were chosen randomly from a Maxwell–Boltzmann distribution in a way that ensured that the system had no net initial momentum. Newton's equations of motion were then integrated at constant energy using fourth-order Gear predictor–corrector methods with periodic boundary conditions and nearest-neighbor lists. Forces between the atoms were described using a two-body Born–Mayer–Huggins potential and a three-body Stillinger–Weber type (Feuston & Garofalini, 1988). The bulk silica structure was annealed to its lowest energy form at room temperature by a melt-quench sequence. The initial configuration was melted at 6000 K by periodic velocity scaling during the first 3000 molecular dynamics (MD) time steps followed by a 7 ps constant energy run. The system was cooled stepwise to 300 K, while ensuring internal equilibrium at intermediate temperatures (4000, 2000, and 1000 K), and then it was run at constant energy for 17 ps at 1000 K in order to ensure complete relaxation before a final quench to 300 K. After a 7 ps equilibration at 300 K, radial distribution functions and bond angles were calculated by collecting the results of the MD simulations for up to 20,000 fs. Simulations were performed using 100–3600 atoms with a 0.001 ps time step at a constant density of 2.20 g/cm³, which corresponds to the bulk density of amorphous silica. The specific number of atoms in each simulation was chosen so that surface diffusivities varied by less than 5% with a twofold increase in the sample size.

2.2. Interatomic potential energy functions

The interactions between atoms in the system were described using both a two-body Born–Mayer–Huggins potential (v_2) and a three-body Stillinger–Weber-type potential (v_3):

$$V = \sum_{i < j} v_2(r_i, r_j) + \sum_{i < j < k} v_3(r_i, r_j, r_k), \quad (1)$$

where V is the total potential energy and r_i, r_j, r_k are the atomic positions of the atoms in each pair or triplet. The two-body potential consists of two terms:

$$v_2(r_{ij}) = A_{ij} \exp\left(\frac{-r_{ij}}{\rho}\right) + \frac{Z_i Z_j e^2}{r_{ij}} \operatorname{erfc}\left(\frac{r_{ij}}{\beta_{ij}}\right), \quad (2)$$

where r_{ij} is the separation distance, e is the unit proton charge, Z_i is the formal ionic charge, and A_{ij} and β_{ij} are adjustable parameters. The first term is a Born–Mayer repulsive term. The second term is an approximate description of long-range attractive Coulombic interactions. For amorphous materials, which lack long-range crystallinity, the attractive forces can be accurately described by local, short-range forces (5–6 Å), which are

approximated by a form of Ewald's sums (Woodcock, Angell, & Cheeseman, 1976; Soules, 1979; Garofalini & Melman, 1986; Feuston & Garofalini, 1988). Silica, however, is not a purely ionic solid and Si–O bonds have a clear covalent and directional nature. Hence, three-body angle-bending terms are added to the potential; they discourage significant deviations from the tetrahedral Si–O–Si and O–Si–O angles (Feuston & Garofalini, 1988; Vessal, Leslie, & Catlow 1989).

The three-body potential was developed by Feuston and Garofalini (1988) and it is based on the three-body potential developed by Stillinger and Weber (1985) for silicon. The form of these additional potential terms is shown below:

$$v_3(r_i, r_j, r_k) = h(r_{ij}, r_{ik}, \theta_{jik}) + h(r_{jk}, r_{ji}, \theta_{kji}) + h(r_{ki}, r_{kj}, \theta_{ikj}), \quad (3)$$

$$h(r_{ij}, r_{ik}, \theta_{jik}) = \begin{cases} \lambda_i \exp\left(\frac{\gamma_i}{r_{ij} - r_i^c}\right) \\ (\cos \theta_{jik} - \cos \theta_{jik}^c)^2, & r_{ij} < r_{ij}^c \text{ and } r_{ik} < r_{ik}^c, \\ 0, & r_{ij} \geq r_{ij}^c \text{ or } r_{ik} \geq r_{ik}^c, \end{cases} \quad (4)$$

where r_{ij}, r_{ik}, r_{jk} are the interatomic separation distances; $r_{ij}^c, r_{ik}^c, r_{jk}^c, \theta_{kji}^c, \theta_{jik}^c, \theta_{ikj}^c$ are cut-off constants; and $\lambda_i, \lambda_j, \lambda_k, \gamma_i, \gamma_j, \gamma_k$ are adjustable parameters. The parameter values used are shown in Tables 1 and 2; they were obtained by Feuston and Garofalini (1988) based on comparisons of the simulated and experimental radial distribution functions obtained by X-ray scatter (Mozzi & Warren, 1969) and neutron scattering (Misawa, Price, & Susuki, 1980).

3. Silica surface simulations

3.1. Methods

3.1.1. Unrelaxed surfaces

Surfaces were created by cutting the simulated bulk silica to the desired geometry. Planar surfaces were generated by removing the periodic boundary condition in one direction. The dangling oxygen bonds that form when siloxane bridges are cleaved become the hydroxyl groups present on the surface of silica materials prepared by abrupt interruption of particle growth in gaseous or aqueous media. A similar approach was used by MacElroy and Raghavan (1990, 1991) in order to create silica microspheres, from which they removed all tri-silanol groups (Si bonded to three OH groups), which are not present on SiO₂ surfaces, by removing the corresponding Si atom

Table 1
Born–Mayer–Huggins potential parameters (Feuston & Garofalini, 1988)

$A_{\text{Si-O}}$ ($\times 10^{-9}$ ergs)	$A_{\text{O-O}}$	$A_{\text{Si-Si}}$	$\beta_{\text{Si-O}}$ (\AA)	$\beta_{\text{O-O}}$	$\beta_{\text{Si-Si}}$
2.96	0.72	1.88	2.55	2.53	2.60

Table 2
Parameter values for the three-body Stillinger–Weber-type potential (Feuston & Garofalini, 1988)

$\lambda_{\text{Si}} = 18.0 \times 10^{-11}$ ergs	$\lambda_8 = 0.3 \times 10^{-11}$ ergs
$\gamma_{\text{Si}} = 2.6$ \AA	$\gamma_{\text{Si}} = 0.6$ \AA
$r_{\text{Si}}^c = 3.0$ \AA	$r_{\text{Si}}^c = 2.60$ \AA
$\cos \theta_{\text{O-Si-O}}^c = -1/3$	$\cos \theta_{\text{Si-O-Si}}^c = -1/3$

and the three associated O atoms. The resulting surfaces were not allowed to relax after cutting (MacElroy & Raghavan, 1990), but the authors concluded that this approach led to a realistic surface based on the similarity between the simulated concentration of surface hydroxyl groups (6.3 OH/nm²) and the values obtained from spectroscopic measurements of silica surfaces (2–7 OH/nm²) (Iler, 1979).

3.1.2. Relaxed surfaces

The unique position of a surface as the interface between the bulk solid and a gas or liquid phase leads to structures and chemical properties that differ from those within the bulk solid. Therefore, simulated surfaces created by fracturing the solid must be allowed to relax to their minimum energy if they are to reflect accurately silica surfaces. Relaxed surfaces were created by allowing atoms in the fractured solid to move under the influence of the same forces used in bulk solid simulations. Surface relaxation was carried out using a method developed by Feuston and Garofalini (1989). In this method, the bottom section of atoms (10%) in a fractured bulk solid sample was fixed and the system allowed to relax at high temperatures (6000 K). The system was then cooled to 300 K in steps, as in the bulk simulation, at which point additional atoms were immobilized (in ~10% increments) until about 50% of the total atoms were fixed.

3.1.3. Random surfaces

The significant effort required in order to perform rigorous MD simulations of silica surfaces led us to examine the accuracy of simpler random surface models by comparing their predictions with those from the MD simulations. A two-step method involving bulk and surface generation steps was used. A bulk solid was created by placing atoms at random positions instead of locating

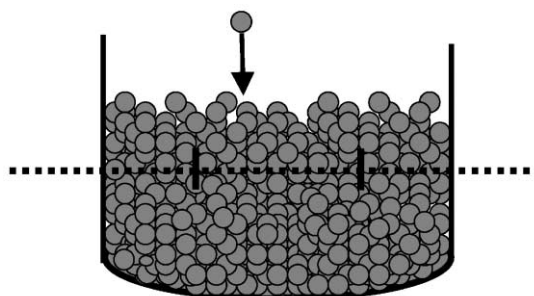


Fig. 1. Generation of a random surface from a Monte Carlo packing of spheres.

them at positions determined by intermolecular potential energy functions. Adsorbates were assumed to interact only with the oxygen atoms in the structure. Hence, only the positions of the oxygen atoms were specified. Their positions were assigned using Monte Carlo methods, in which spheres (oxygen atoms) were dropped randomly into a large cylindrical container and allowed to fall until they reached a stable three-point contact (Jodrey & Tory, 1981). The code was adapted from one reported previously to describe pore structures in random mesoporous solids (Reyes & Iglesia, 1991). The sphere size was chosen in order to match the first peak in the radial distribution function with the experimental O–O distance (1.61 \AA) (Mozzi & Warren, 1969; Misawa, Price, & Susuki, 1980). This packing was then fractured at a random position, keeping all atoms located below the fracture line. Only the atoms within the central portion of the cylindrical container were included in order to avoid wall effects on the packing density. A schematic of this process to generate this random silica surface is shown in Fig. 1.

3.1.4. Ordered surface

Finally, a simple ordered surface was also considered. The crystalline silica polymorph, α -cristobalite, was created by repeating multiple unit cells with atomic positions obtained from reported crystal structure data (Hyde & Andersson, 1989). An ordered surface was then created by fracturing the α -cristobalite structure and keeping all of the oxygens bound to the silicon atoms located near the surface.

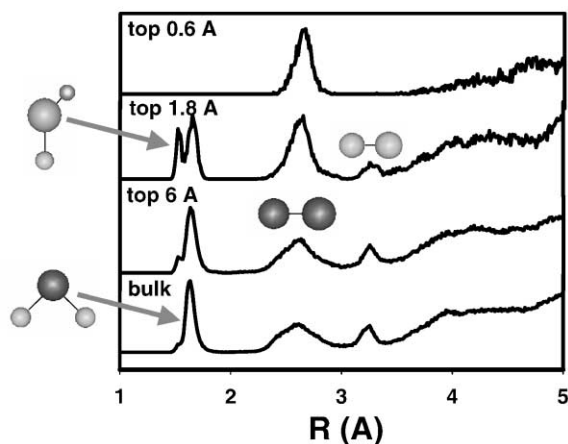


Fig. 2. Radial distribution functions as a function of distance from the silica surface.

3.2. Surface structure results

The geometric properties of the surfaces generated by the different methods were examined first. The concentrations of surface hydroxyl groups (non-bridging oxygens) obtained on simulated surfaces were compared to experimental values. The ordered surface, α -cristobalite re-scaled to the density of amorphous silica (2.2 g/cm^3), had a surface hydroxyl concentration of 8 OH per nm^3 . The relaxed and unrelaxed surfaces had surface hydroxyl concentrations of 6–7 OH per nm^2 when fractured. No corresponding values were calculated for the random surfaces, which do not contain the structural silicon portion needed for the calculation. These values lie at the high end of the experimental OH surface density range (4.2–6.2 OH per nm^2), which varies depending on thermal treatment of the samples after synthesis (Iler, 1979; Zhuravlev, 1987).

Radial distribution functions were obtained as a function of distance from the surface. Fracture without relaxation leads to bulk-like radial distribution functions at all distances from the surface. Only the presence of surface dangling oxygen bonds, created by cleaving Si–O–Si bonds, distinguishes the geometric and chemical features of the surface from those in the bulk of silica particles.

Radial distribution functions for relaxed surfaces, however, vary with distance from the surface. Relaxation of simple planar cuts leads to a shorter Si–O distance (1.5 Å) near the surface, corresponding to the shorter Si–O distance for terminal oxygens, in agreement with previous work (Feuston & Garofalini, 1989). A more detailed analysis by Feuston and Garofalini (1989) and the simulated radial structure functions shown in Fig. 2 show that the relaxed surface also contains a higher density of defects (over and under coordinated silicon and oxygen atoms) and of small rings containing 2–4 silicon atoms instead of the six silicon rings typical of bulk silica.

Surface geometry, by itself, cannot be used to establish the fidelity of these simulated surfaces, because it is not possible to measure such details of the surface structure in amorphous materials. The energetics and connectivity of such surfaces, however, can be characterized by their chemical interactions with specific molecules during adsorption–desorption and by the dynamics with which the adsorbed species diffuse. In the next section, surface thermodynamic properties were probed by estimating heats of adsorption and comparing them with experimental results and by simulating the dynamics of surface diffusion.

4. Heats of adsorption

4.1. Method

In order to investigate the interactions of adsorbed species with surfaces, we require a potential energy function that describes accurately such interactions. With the development of quantum mechanical methods, these energy functions are increasingly being obtained from ab initio treatments (Wiesenekker, Kroes, & Baerends, 1996; Sorescu & Yates, 1998). Such potential energy functions, however, are not yet available to describe interactions between small molecules and surfaces. For clean, single-crystal metal surfaces, scattering measurements with angular distributions and energy transfer data at multiple incidence angles can be used to develop empirical potential energy functions (Cardillo, 1985; Barker & Rettner, 1992). This method cannot be applied to amorphous surfaces. Therefore, we must use instead an interaction potential with parameters available from accessible data, such as atomic size and polarizability and Henry's adsorption constants. Here, we use a Lennard–Jones-type potential energy function:

$$v_2(r_{ij}) = 4\epsilon \left[\left(\frac{\sigma}{r_{ij}} \right)^{12} - \left(\frac{\sigma}{r_{ij}} \right)^6 \right], \quad (5)$$

where r_{ij} is the separation distance between the molecule and a surface atom and σ and ϵ are adjustable parameters. Lennard–Jones parameters are available in the literature for interactions between silica and various small molecules (MacElroy & Raghavan, 1990; Kohler & Garofalini, 1994). Adsorbed molecules can interact with terminal oxygen atoms in hydroxyl groups, with oxygens in siloxane bridges, or with silicon atoms. The interaction with silicon atoms is very weak ($\epsilon \sim 0.1 \times 10^{-14}$ ergs) (Kohler & Garofalini, 1994). Interactions with the two types of oxygens were either assumed to be equivalent, or a larger size parameter was used in the potential to account for the larger size of the hydroxyl oxygen. Values used in the calculations are shown in Table 3.

Table 3
Lennard–Jones potential parameters for surface oxygen-adsorbate interactions

	σ (Å)	ϵ (erg $\times 10^{-14}$)	Reference
N ₂	3.2175	2.7813	(Kohler & Garofalini, 1994)
Ar	3.070	3.1217	(Kohler & Garofalini, 1994)
CH ₄	3.2 (bridging oxygen)	2.5410	(MacElroy & Raghavan, 1990)
	3.35 (non-bridging oxygens)	2.5410	(MacElroy & Raghavan, 1990)

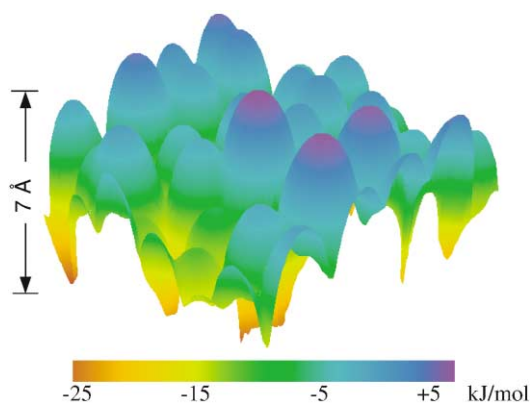


Fig. 3. Potential energy surface for N₂ on a relaxed simulated silica surface.

4.2. Results

4.2.1. Potential energy surfaces

Interaction energies between molecules and surfaces were calculated by placing the molecule above the surface (6–10 Å depending upon the surface topology), calculating the potential energy, and then decreasing the distance between the molecule and the surface in small increments (0.1–0.001 Å) until the energy reached a minimum value (i.e. when energies for three consecutive steps decreased and then increased again). Potential energy surfaces were obtained by dividing the surface into a grid (0.2 Å) and repeating this calculation at each grid point. The potential energy surface for N₂ on a relaxed silica surface is shown in Fig. 3. It shows a non-uniform distribution of adsorption energies with well-defined adsorption sites located at the bottom of the energy wells. The corresponding topological energy contour map is shown in Fig. 4. The energy contour plot for N₂ on an unrelaxed silica surface is shown in Fig. 5. The calculation process was slightly different for the random surface, because it was not periodic. In this case, minimum energies were calculated using the same procedure as for MD-generated surfaces but only for the central regions of larger surfaces. The resulting potential energy surface for N₂ on a random surface is shown in Fig. 6. For comparison, the potential energy surface for the ordered surface created from α -cristobalite is also shown (Fig. 7).

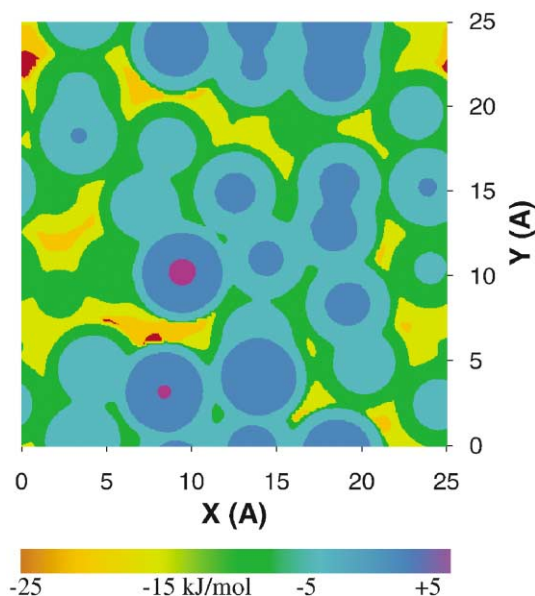


Fig. 4. Potential energy contour plot for N₂ on a relaxed simulated silica surface.

The relaxed silica surface (Figs. 3, 4) has richer features and better defined peaks and valleys than unrelaxed surfaces (Fig. 5). Random surfaces (Fig. 6) show more localized and better-defined adsorption sites than unrelaxed surfaces (Fig. 5), but they also show much flatter potential energy surfaces, which lack the high- and low-energy values observed for relaxed silica surfaces (Fig. 3). In contrast, the ordered surface (Fig. 7) possesses only one type of adsorption site with regular connectivity among identical sites; the potential energy surfaces are flatter than those for the other surfaces. The surface properties and non-uniformity of these surfaces can be quantitatively compared using the adsorption energy distributions described in the next section.

4.2.2. Adsorption energy distributions

The distribution of adsorption energies on a given surface was obtained from the potential energy surface by determining the energy values at the bottom of each potential energy well. These minima were obtained by comparing the energy value of each grid point on the potential energy surface (points spaced ever 0.2 Å) to its

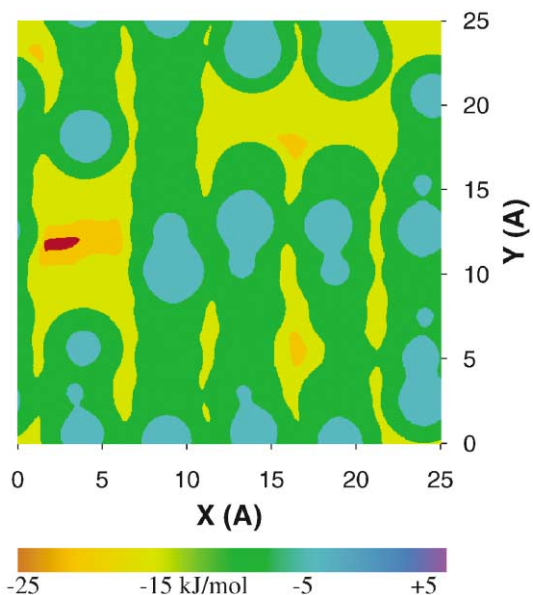


Fig. 5. Potential energy contour plot for N_2 on an unrelaxed simulated silica surface.

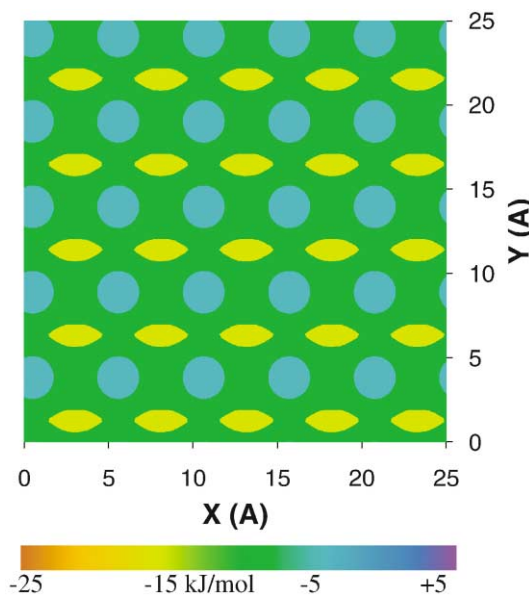


Fig. 7. Potential energy contour plot for N_2 on an ordered simulated silica surface.

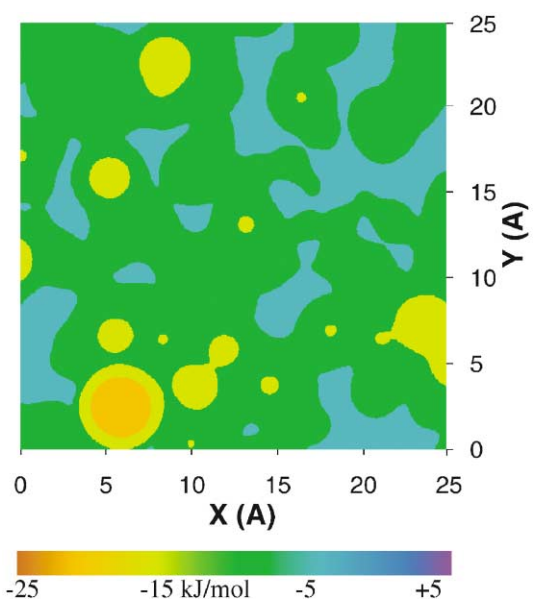


Fig. 6. Potential energy contour plot for N_2 on a random simulated silica surface.

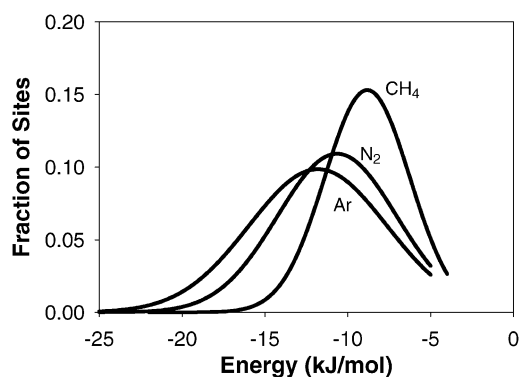


Fig. 8. Adsorption energy distributions for N_2 , CH_4 , and Ar on a relaxed simulated silica surface.

eight adjacent grid points (2 vertical, 2 horizontal, and 4 diagonal points). If the energy value was lower than the values at all eight other points, that grid point was denoted as a minimum. Minimum energies were calculated for ten different ($25 \text{ \AA} \times 25 \text{ \AA}$) relaxed and unrelaxed surfaces and for one ($150 \text{ \AA} \times 150 \text{ \AA}$) random surface. Adsorption energy distributions for N_2 , CH_4 , and Ar on relaxed silica surfaces are shown in Fig. 8. The average heats of adsorption for each type of molecule were obtained

by fitting adsorption energy distributions on ten different relaxed surfaces to a Gaussian distribution. The resulting adsorption energies on relaxed simulated surfaces are compared to experimental values in Table 4. The average value for CH_4 adsorption on relaxed silica surfaces is within 0.2 kJ/mol of experimental values reported previously (Gangwal, Hudgins, & Silveston, 1979). The average values for N_2 and Ar are within 2 kJ/mol of their corresponding experimental values. The differences among these molecules in the agreement between calculated and experimental heats of adsorption reflect the method used in order to obtain the Lennard–Jones parameters required for each molecule. CH_4 values were obtained by fitting simulation results for unrelaxed surfaces to experimental Henry law constants; thus, ensuring agreement of the simulations with experiment (MacElroy

Table 4
Average heats of adsorption on silica

	ΔH_{ads} (kJ/mol) simulated	ΔH_{ads} (kJ/mol) experimental	Reference
N ₂	11.9	10.2	(Brunauer, Emmett, & Teller, 1938)
Ar	13.1	11.5	(Brunauer, Emmett, & Teller, 1938)
CH ₄	10.5	10.6	(Gangwal, Hudgins, & Silveston, 1979)

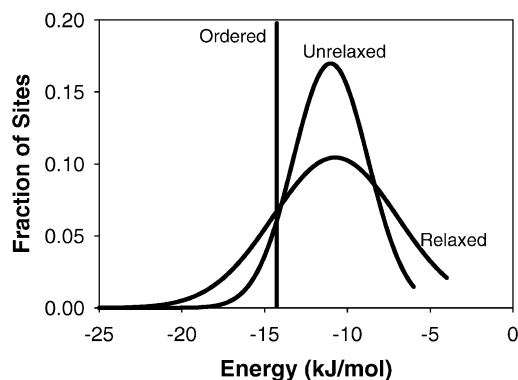


Fig. 9. Adsorption energy distributions for N₂ on various types of simulated silica surfaces.

& Raghavan, 1990). Therefore, excellent agreement is expected. The parameters for Ar and N₂, however, were extrapolated from those reported for zeolite systems.

Adsorption energy distributions were also calculated for N₂ on the various types of simulated silica surfaces (Fig. 9). The ordered system has only one type of minimum energy site, and hence, a single adsorption energy (14.3 kJ/mol). The surfaces created by the molecular dynamics and Monte Carlo methods, however, show sites with a range of binding energies. Similar average adsorption energies were obtained on the relaxed (11.9 kJ/mol) and unrelaxed (11.4 kJ/mol) surfaces, and a slightly higher value was obtained on the random surface (12.8 kJ/mol). Relaxed surfaces led to broader distributions than unrelaxed surfaces. Relaxed surfaces have weaker and stronger binding sites than unrelaxed surfaces, as expected from their more rugged potential energy surfaces (Figs. 4 and 5). The breadth of the adsorption energy distribution for the unrelaxed surface is similar to that obtained for random surfaces, even though they have very different energy topology and markedly different connectivity among adsorption sites.

The features of the actual amorphous surface seem to be represented most accurately by the relaxed surface obtained from molecular dynamics simulations. This surface possesses a distribution of energy sites with non-uniform distribution, in contrast to the single adsorption site energy present on the ordered surface or the channels

evident in the potential energy surface of the unrelaxed surface. The random surface, which also possesses a distribution of sites with random connectivity, has a higher heat of adsorption than experimentally found (10.2 kJ/mol) (Brunauer, Emmett, & Teller, 1938).

5. Surface diffusion

5.1. Method

Adsorption measurements and simulations probe the distribution of energy binding sites on the surface, but they provide no information about the connectivity between these sites. Measurements of the dynamics of molecules diffusing on the surface, however, reflect the binding energy and the connectivity of surface sites. As a result, surface diffusivities are more sensitive to the chemical and geometric details of the surface than binding energies. Unfortunately, experimental surface diffusion measurements are scarce. In this paper, the dynamic properties of simulated silica surfaces were probed by comparing the diffusional behavior of adsorbates on each surface. Specifically, the migration of weakly bound molecules, such as N₂ was followed using molecular dynamics methods that explicitly solve the equations of motion for these migrating species on each surface. In these calculations, surface atom positions were fixed from the previous simulations, and only the adsorbed species were allowed to move. This simplification is appropriate for weakly interacting adsorbates, which exchange little energy with the surface (Utrera & Ramirez, 1992). Indeed, the diffusivity estimates obtained from our static surface simulations were within 5–10% of those in which the top layers of the surface were allowed to relax during migration of adsorbed species. The adsorbates were placed randomly at a height of 3–8 Å above the surface. This distance depended upon the roughness of the surface, and it was chosen to minimize the frequent initial desorption of molecules placed near the surface. Simulations were carried out using the same technique outlined for the bulk simulations, except at constant temperature instead of energy, because of the nature of the dynamic system being examined, in which potential and kinetic energies can fluctuate but the temperature is kept constant. Interactions between adsorbed

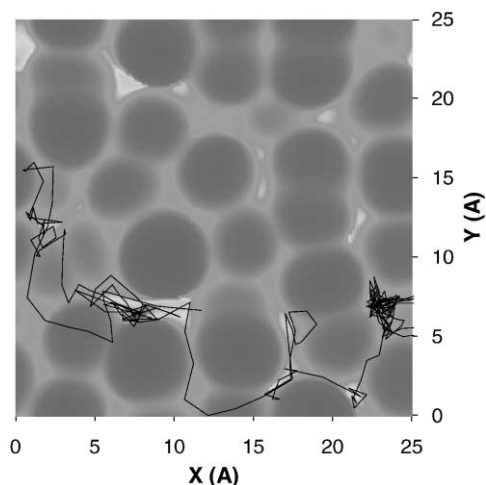


Fig. 10. Trajectory plot of N_2 molecule diffusing on a relaxed simulated silica surface (100 fs).

species and surface atoms were calculated using the Lennard–Jones potential used in the adsorption calculations. The surface diffusivity was calculated using two methods. In one method, the Einstein diffusion equation in two-dimensions:

$$\langle R^2 \rangle = 4D_s t, \quad (6)$$

was used, where $\langle R^2 \rangle$ is the mean-squared displacement of a molecule, D_s is the surface diffusion coefficient, and t is the elapsed time. Another method used the velocity-autocorrelation functions:

$$D_s = \int_0^\infty \frac{1}{2} \langle (v_x(t)v_x(0) + v_y(t)v_y(0)) \rangle dt, \quad (7)$$

where v_x and v_y are the velocity components in the x and y directions at time 0 or time t (Riccardo & Steele, 1996). In this method, diffusivities are obtained from the dynamics of the short-term randomization of the initial velocity vector for a given set of molecules. Activation energies for surface diffusion were calculated assuming that surface diffusion is an activated process that can be described accurately by an Arrhenius equation:

$$D_s = D_0 e^{-E_a/RT}, \quad (8)$$

where D_s is the surface diffusivity (cm^2/s), D_0 is the pre-exponential factor (cm^2/s), E_a is the activation energy for surface diffusion (kJ/mol), R is the universal gas constant ($\text{kJ}/\text{mol K}$), and T is the temperature (K).

5.2. Results

A typical trajectory for N_2 migration on a relaxed silica surface is shown in Fig. 10. Molecules diffuse predominantly by following the lowest energy paths across the surface. Surface diffusivities obtained for each surface at 200–300 K are shown in Fig. 11. The rate of surface diffusion was slowest on relaxed surfaces. Although they

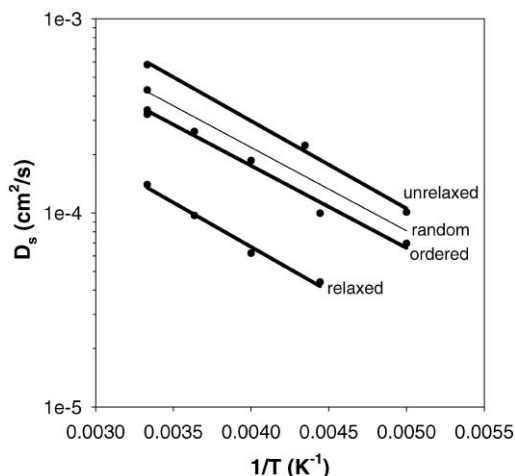


Fig. 11. Arrhenius surface diffusion plots obtained for adsorbed N_2 on various types of simulated silica surfaces.

do not have the highest average adsorption energy, relaxed surfaces show the broadest distribution of adsorption energies and the sites with the strongest binding sites among all surfaces examined. Diffusion was fastest on unrelaxed surfaces, which have a similar average adsorption energy, but a narrower range of adsorption energies. Surface diffusion was also faster on ordered and random surfaces than on relaxed surfaces; although both ordered and random surfaces have higher average adsorption energies, they lack the stronger binding sites present on relaxed surfaces.

Surface diffusion rates on the random, unrelaxed, and ordered surfaces are more similar to each other than to the values obtained for relaxed surfaces. The difference in surface diffusivities between these systems reflects a subtle balance between the average adsorption properties of the surface and the distribution in both energy and connectivity among these adsorption sites. The ordered system has the highest average binding energy among the surfaces examined, a feature that leads to slower diffusional processes. But the regular arrangement of binding sites prevents the stranding of molecules in unconnected or poorly connected regions of the surface. Random and unrelaxed surfaces contain some binding sites stronger than in the ordered surfaces, but fewer than in relaxed surfaces. The density of unconnected regions, however, is smaller than on the relaxed surfaces and the surface diffusivities consequently larger. Diffusion is fastest on the unrelaxed surface which has the smallest average adsorption energy and whose potential energy surface exhibited “channels” between energy sites, which can enhance diffusion compared to the more randomly connected sites present on random or relaxed surfaces.

The relaxed surface showed the largest diffusion activation energy (7.8 kJ/mol); this value equals 0.65 of the average adsorption energy. Activation energies on the unrelaxed, random, and ordered surfaces were smaller

(7.0, 7.0, and 6.9 kJ/mol) than on the relaxed surfaces, reflecting the flatter potential energy surfaces shown in Figs. 5–7 and the balance between the depth and the connectivity of the minima in the potential energy surface.

Unfortunately, experimental surface diffusivities are scarce for well-characterized amorphous surfaces. Reported surface diffusivities for weakly bound molecules on silica glasses are in the range of 10^{-2} – 10^{-4} cm²/s (Sladek, Gilliland, & Baddour, 1974; Tamon, Okazaki, & Toei, 1985). Experimental surface diffusivities for CH₄, N₂, and Ar on Vycor glass are similar ($\sim 2 \times 10^{-4}$ cm²/s) at 300–350 K and they show similar activation energies (6 kJ/mol) (Barrer, Gabor, & Gabor, 1959). These values are within the range obtained by the simulations of these molecules on silica. The agreement is encouraging, because the dynamic simulations were based on Lennard–Jones parameters based exclusively on thermodynamic data (adsorption constants). Slightly higher activation energies were obtained in the simulations, which could be indicative of the greater disorder of the amorphous silica surfaces compared with the surface of Vycor glass.

Even though the simulated surface diffusivities lie within the range of experimental values, the selection of one type of theoretical surface description over another cannot be made rigorously without additional experimental data. Slower diffusion (up to a factor of four) was obtained on relaxed surfaces than on the others, and indeed such relaxed surfaces seem to be the most appropriate and representation of actual amorphous surfaces formed by the abrupt interruption of particle growth in gaseous or aqueous media. Differences among surface diffusivities obtained on the ordered, random, and unrelaxed surfaces were smaller.

6. Conclusions

Increasing the level of detail and of complexity used to describe silica surfaces leads to more faithful descriptions of the heterogeneous nature of the surfaces and to the appearance of adsorption sites with the experimentally found adsorption energies and with the expected random connectivity among adsorption sites. Potential energy contours for relaxed surfaces showed greater heterogeneity than those for unrelaxed, random, or ordered surfaces, and a wider range of adsorption site energies. Similar average heats of adsorption were obtained for the random, relaxed, and unrelaxed surfaces. The relaxed and random surfaces, however, showed more random adsorption site connectivity, in contrast with the regular connectivity of ordered surfaces or the more distinct low-energy channels on unrelaxed surfaces. As expected, surface diffusion on relaxed surfaces was slower and showed a higher activation energy than on the other surfaces because their more non-uniform site distributions led to

deeper energy wells and to unconnected or poorly connected surface regions in which molecules can remain for long periods of time. Ordered, random, and unrelaxed surfaces, although possessing different adsorption properties, had very similar surface diffusivities and diffusion activation energies, in spite of the varying level of complexity used in their synthesis. Surface diffusivities on simplest (ordered) surface were closest in value to those obtained on the most complex (relaxed) surfaces, even though the adsorption distribution of the relaxed surface resembled most closely that of the random surface. From a geometric and chemical point of view, the relaxed surface seems to be the best representation of the amorphous silica surface. In light of the meager surface diffusivity data, it is not possible at this time to reach a definite conclusion that the relaxed surfaces, although more rigorous and appropriate, provide the best representation of silica surfaces treated at low temperatures.

Notation

A_{ij}	adjustable parameter in BMH two-body potential, kJ
D_0	pre-exponential factor in Arrhenius expression for surface diffusion, cm ² /s
D_s	surface diffusivity, cm ² /s
D_f	fractal dimension
e	unit proton charge
E_a	activation for surface diffusion, kJ/mol
h	functional term in three-body potential
r_i, r_j, r_k	atomic position of atom, i, j, k , in each pair or triplet r_{ij} separation distance between two atoms or a molecule and an atom, Å
r_{ik}	interatomic separation distance between atoms i and k , Å
r_{jk}	interatomic separation distance between atoms j and k , Å
r_{ij}^c	cut-off constant in three-body potential, Å
r_{ik}^c	cut-off constant in three-body potential, Å
r_{jk}^c	cut-off constant in three-body potential, Å
\bar{R}	universal gas constant, kJ/mol K
$\langle R^2 \rangle$	mean squared displacement
t	time
T	temperature, K
v_x	velocity component in the x direction
v_y	velocity component in the y direction
V	total potential energy, kJ
Z_i	formal ionic charge

Greek letters

β_{ij}	adjustable parameter in BMH two-body potential, Å
--------------	---

ε	adjustable parameter in Lennard–Jones potential, Å
γ_i	adjustable parameter in three-body potential, Å
γ_j	adjustable parameter in three-body potential, Å
γ_k	adjustable parameter in three-body potential, Å
θ_{kji}^c	cut-off angle in three-body potential
θ_{jik}^c	cut-off angle in three-body potential
θ_{ikj}^c	cut-off angle in three-body potential
λ_t	adjustable parameter in three-body potential, ergs
λ_j	adjustable parameter in three-body potential, ergs
λ_k	adjustable parameter in three-body potential, ergs
v_2	two-body potential energy, kJ
v_3	three-body potential energy, kJ
σ	adjustable parameter in Lennard–Jones potential, Å

7. Acknowledgements

The authors thank Dr. Sebastian Reyes of Exxon Research and Engineering for the Monte Carlo code used to generate the random sphere packings. The authors also acknowledge useful technical discussions with Dr. Joachim Jacobsen from Haldor Topsoe A&S and financial support from Haldor Topsoe A&S. One of the authors (J.M.S.) gratefully acknowledges fellowship support from the National Science Foundation and from the Shell Education Foundation.

References

- Athanasopoulos, D. C., & Garofalini, S. H. (1992). Molecular dynamics simulations of the effect of adsorption on SiO₂ surfaces. *Journal of Chemical Physics*, *97*(5), 3775–3780.
- Bakaev, V. A. (1999). Continuous random networks at the silica surface. *Physical Review B*, *60*, 10723.
- Bakaev, V. A., & Steele, W. A. (1992). Computer simulation of the adsorption of argon on the surface of titanium dioxide. 2. Amorphous Surface. *Langmuir*, *8*, 1379–1384.
- Bakaev, V. A., & Steele, W. A. (1999a). On the computer simulation of a hydrophobic vitreous silica surface. *Journal of Chemical Physics*, *111*(21), 9803–9812.
- Bakaev, V. A., & Steele, W. A. (1999b). On the computer simulation of a hydrophobic vitreous silica surface. *Journal of Chemical Physics*, *111*(21), 9813–9821.
- Barker, J. A., & Rettner, C. T. (1992). Accurate potential energy surface for Xe/Pt(111): A benchmark gas/surface interaction potential. *Journal of Chemical Physics*, *97*(8), 5844–5850.
- Barrer, R. M., Gabor, F. R. S., & Gabor, T. (1959). A comparative structural study of cracking catalyst, porous glass, and carbon plugs by surface and volume flows of gases. *Proceedings of the Royal Society of London, Series A*, *251*, 353–368.
- Benegas, E. I., Pereyra, V. D., & Zgrablich, G. (1987). On the behavior of adsorption isotherms of a Lennard–Jones Gas on a disordered lattice. *Surface Science*, *187*(1), L647–L653.
- Bojan, M. J., & Steele, W. A. (1988). Computer simulation of physisorption on a heterogeneous surface. *Surface Science*, *199*(3), L395–L402.
- Brunauer, S., Emmett, P. H., & Teller, E. (1938). Adsorption of gases in multimolecular layers. *Journal of the Chemical Society*, *60*, 309–319.
- Cardillo, M. J. (1985). Concepts in gas-surface dynamics. *Langmuir*, *1*, 4–10.
- Drewry, H. P. G., & Seaton, N. A. (1995). Continuum random walk simulations of diffusion and reaction in catalyst pellets. *A.I.Ch.E. Journal*, *41*(4), 880–893.
- Feuston, B. P., & Garofalini, S. H. (1988). Empirical three-body potential for vitreous silica. *Journal of Chemical Physics*, *89*(9), 5818–5824.
- Feuston, B. P., & Garofalini, S. H. (1989). Topological and bonding defects in vitreous silica surfaces. *Journal of Chemical Physics*, *91*(1), 564–570.
- Feuston, B. P., & Garofalini, S. H. (1990). Water-induced relaxation of the vitreous silica surface. *Journal of Applied Physics*, *68*(9), 4830–4836.
- Finney, J. L. (1983). Modelling of atomic structure. In F. E. Luborsky (Ed.), *Amorphous metallic alloys* (p. 42). London: Butterworths.
- Gangwal, S. K., Hudgins, R. R., & Silveston, P. L. (1979). Reliability and limitations of pulse chromatography in evaluating properties of flow systems I. Modeling and experimental considerations. *Canadian Journal of Chemical Engineering*, *57*(5), 609–620.
- Garofalini, S. H., & Melman, H. (1986). Applications of molecular dynamics simulations to sol–gel processing. In C. J. Brinker, D. E. Clark, & D. R. Ulrich (Eds.), *Better ceramics through chemistry II: MRS symposium proceedings*, Vol. 73 (p. 497). Pittsburgh: Materials Research Society.
- Gomer, R. (1990). Diffusion of adsorbates on metal surfaces. *Reports on Progress in Physics*, *53*(7), 917–1002.
- Haus, J. W., & Kehr, K. W. (1987). Diffusion in regular and disordered lattices. *Physics Reports*, *150*(5–6), 264–406.
- Hyde, B. G., & Andersson, S. (1989). *Inorganic crystal structures*. New York: Wiley.
- Iler, R. K. (1979). *The chemistry of silica*. New York: Wiley.
- Jodrey, W. S., & Tory, E. M. (1981). Computer simulation of isotropic, homogeneous, dense random packing of equal spheres. *Powder Technology*, *30*(2), 111–118.
- Keil, F. J. (1996). Modelling of phenomenon within catalyst particles. *Chemical Engineering Science*, *51*(10), 1543–1567.
- Kohler, A. E., & Garofalini, S. H. (1994). Effect of composition on the penetration of inert gases adsorbed onto silicate glass surfaces. *Langmuir*, *10*(12), 4664–4669.
- Litton, D. A., & Garofalini, S. H. (1997). Vitreous silica bulk and surface self-diffusion analysis by molecular dynamics. *Journal of Non-Crystalline Solids*, *217*, 250–263.
- MacElroy, J. M. D., & Raghavan, K. (1990). Adsorption and diffusion of a Lennard–Jones vapor in microporous silica. *Journal of Chemical Physics*, *93*(3), 2068–2079.
- MacElroy, J. M. D., & Raghavan, K. (1991). Transport of an adsorbing vapour in a model silica system. *Journal of the Chemical Society—Faraday Transactions*, *87*(13), 1971–1987.
- Misawa, M., Price, D. L., & Susuki, K. (1980). Short range structure of alkali disilicate glasses by pulse neutron total scattering. *Journal of Non-Crystalline Solids*, *37*(1), 85–97.
- Mozzi, R. L., & Warren, B. E. (1969). The structure of vitreous silica. *Journal of Applied Crystallography*, *2*, 164–172.
- Nicholson, D., & Silvester, R. G. (1977). Investigation of step formation in multilayer adsorption isotherms using a lattice model. *Journal of Colloid Interface Science*, *62*(3), 447–453.

- O'Brien, J. A., & Myers, A. L. (1985). Physical adsorption of gases on heterogeneous surfaces—Model study of the effects of simultaneous vertical and lateral interactions by Monte Carlo methods. *Journal of Chemical Society—Faraday Transactions*, 81, 355–373.
- Reyes, S. C., & Iglesia, E. (1991). Effective diffusivities in catalyst pellets: New model porous structures and transport simulation techniques. *Journal of Catalysis*, 129, 457–472.
- Reyes, S. C., & Iglesia, E. (1993). Simulation techniques for the characterization of structural and transport properties of catalyst pellets. In E. R. Becker, & C. J. Pereira (Eds.), *Computer-aided design of catalysts* (p. 89). New York: Marcel Dekker, Inc.
- Riccardo, J. L., & Steele, W. A. (1996). Molecular dynamics study of tracer diffusion of argon adsorbed on amorphous surfaces. *Journal of Chemical Physics*, 105(21), 9674–9685.
- Rudzinski, W., & Everett, D. H. (1992). *Adsorption of gases on heterogeneous surfaces*. London: Academic Press Ltd.
- Sladek, K. J., Gilliland, E. R., & Baddour, R. F. (1974). Diffusion on surfaces 2. Correlation of diffusivities of physically and chemically adsorbed gases. *Industrial and Engineering Chemistry Fundamentals*, 13, 100–105.
- Sorescu, D. C., & Yates, J. T. (1998). Adsorption of CO on the TiO₂(110) surface: A theoretical study. *Journal of Physical Chemistry B*, 102(23), 4556–4565.
- Soules, T. F. (1979). A molecular dynamics calculation of the structure of sodium silicate glasses. *Journal of Chemical Physics*, 71(11), 4570–4578.
- Steele, W. (1997). Computer simulation of surface diffusion in adsorbed phases. In W. Rudzinski, W. A. Steele, & G. Zgrablich (Eds.), *Equilibria and dynamics of gas adsorption on heterogeneous solid surfaces*, Vol. 104 (p. 451). Amsterdam: Elsevier Science.
- Stillinger, F. H., & Weber, T. A. (1985). Computer simulation of local order in condensed phases of silicon. *Physical Review B*, 31(8), 5262–5271.
- Tamon, H., Okazaki, M., & Toei, R. (1985). Prediction of surface flow coefficient of adsorbed gases on porous media. *A.I.C.H.E. Journal*, 31(7), 1226–1228.
- Utrera, L., & Ramirez, R. (1992). Molecular dynamics simulation of Xe diffusion on the Si(100)-2 × 1 surface. *Journal of Chemical Physics*, 96(10), 7838–7847.
- Vessal, B., Leslie, M., & Catlow, C. R. A. (1989). Molecular dynamics simulation of silica glass. *Molecular Simulation*, 3, 123–136.
- Wiesenekker, G., Kroes, G. J., & Baerends, E. J. (1996). An analytical six-dimensional potential energy surface for dissociation of molecular hydrogen on Cu(100). *Journal of Chemical Physics*, 104(18), 148–158.
- Woodcock, L. V., Angell, C. A., & Cheeseman, P. (1976). Molecular dynamics studies of vitreous state—simple ionic systems and silica. *Journal of Chemical Physics*, 65(4), 1565–1577.
- Zgrablich, G. (1997). Surface diffusion of adsorbates on heterogeneous substrates. In W. Rudzinski, W. A. Steele, & G. Zgrablich (Eds.), *Equilibria and dynamics of gas adsorption on heterogeneous solid surfaces*, Vol. 104 (p. 373). Amsterdam: Elsevier Science.
- Zhuravlev, L. T. (1987). Concentration of hydroxyl groups on the surface of amorphous silicas. *Langmuir*, 1987(3), 316–318.